LAWRENCE
LIVERMORE
NATIONAL
LABORATORY

LLNL-JRNL-410812

Carbonaceous aerosols and the third polar ice cap

S. Menon, D. Koch, G. Beig, S. Sahu, J. Fasullo, D. Orlikowski

February 24, 2009

Atmospheric Chemistry and Physics

Disclaimer

LLNL-JRNL-410812

Carbonaceous aerosols and the third polar ice cap

Surabi Menon,[1*] Dorothy Koch,[2] Gufran Beig,[3] S Sahu,[3]
John Fasullo[4] and Daniel Orlikowski[5]

[1]Lawrence Berkeley National Laboratory,
Berkeley, CA, USA
[2]Columbia University/NASA GISS, New York, NY, USA
[3]Indian Institute for Tropical Meteorology, Pune, India
[4]Climate Analysis Section, CGD/NCAR, Boulder, CO, USA
[5]Lawrence Livermore National Laboratory, Livermore, CA, USA

*To whom correspondence should be addressed; E-mail: smenon@lbl.gov

We examine decadal climate changes (1990 to 2010) over India due to aerosol emissions using a climate model that includes all aerosol (direct and aerosol-cloud) effects including changes to snow/ice albedo from black carbon (BC) deposition. We use two different BC emission inventories for India. New estimates indicate that Indian BC from coal and biofuel are relatively large and transport is expected to expand rapidly in coming years. Over the Himalayas, for 1990 to 2000, simulated snow/ice cover decreases by $\sim$0.9% due to aerosols. The contribution of the enhanced Indian BC to this decline is $\sim$30%, similar to that simulated for 2000 to 2010. Spatial patterns of modeled changes in snow cover and precipitation, similar to observations (for 1990 to 2000), are mainly obtained with the newer BC estimates.

India is a rapidly growing economy with GDP growth at $3 trillion (PPP) for 2007 and

with strong future growth potential. To meet economic demands, power-generation capacity has to increase significantly (*1*). Indian CO_2 emissions rose from over zero billion tonnes to over one in the last 30 years and is expected to reach two billion tonnes by 2030. India also has the world's fourth biggest coal reserve. As expected emissions of GHGs and particulate matter or aerosols have been increasing over the last few decades and are expected to increase in the future as well due to rapid industrial growth and slower emission control measures. Black carbon (BC) aerosols, released from incomplete combustion, have been increasingly implicated as causing large changes in the hydrology, surface radiation, atmospheric heating rates and radiative forcing over Asia (*2, 3*) and its deposition on snow cover is thought to increase snow melt (*4–7*). In India BC from biofuel combustion is highly prevalent (*8, 9*) and compared to other regions, BC aerosol amounts are quite high.

Climate impacts over India from BC aerosols have been studied extensively through the Asian Brown Cloud project (*10–12*). Recent thinning of glaciers over the Himalayas (sometimes referred to as the third polar region (*13*), see Fig.S1 for location) have also raised concern on future water supplies since these glaciers are the main supply of water to ten large river systems that are the lifeline to more than two hundred million people inhabiting the surrounding areas. A recent study has suggested that 915 km^2 of Himalayan glaciers in Spiti/Lahaul (Himachal Pradesh (30-33°N, 76-79°E, India) thinned by an annual average of 0.85 m between 1999-2004 (*14*). Data from the Asian Brown Cloud project (*12*) was used in a modeling study to suggest that the melting of the Himalayan glaciers is related to enhanced heating from BC aerosols and GHGs of 0.25K per decade, from 1950 to present (similar to observations), of which the BC associated heating is 0.12 K per decade. Using Himalayan ice core records a significant amount of BC deposition was found in the Everest region for the 1951-2000 period with strong increases in BC since 1990 (*15*) and observed records of snow cover trends have indicated a sharp decline of $\sim$4% from 1997-2003 (*16*).

To quantify changes to snow/ice cover and precipitation over the Indian subcontinental region due to aerosols (includes sulfates, organic matter (OM) and BC) we analyze their climate impacts for 1990 to 2010. We use the NASA Goddard Institute for Space Studies climate model coupled to an on-line aerosol chemistry/transport model and include the impacts from the aerosol direct effect (DE), aerosol-cloud interactions (IE) and changes to snow/ice albedo from BC deposition (BCA) (*17*). To understand how climate may vary based on changes in emissions for particular decades and also from differences in emission inventories used, we examine various simulations listed in Table 1. All emissions other than carbonaceous aerosols are described in (*17*). For carbonaceous aerosols, emissions are based on (*18*) (referred to as Bond emissions) and additionally we use more recent emissions from (*19*) (referred to as Beig emissions) that differ from the Bond emissions for the Indian region (7.5-37.5° N, 67.5-97.5° E) mainly for contributions to BC from coal, transportation and to some extent biofuel sources. The Beig emissions use emission factors adopted from (*20*) that provides separate emission factors for developed, under developed and developing countries, and these emission factors are higher than that used in (*18*).

As shown in Table 1, BCI_0/BCB_0 and BCI_9/BCB_9 denote simulations that use the Beig/Bond emissions for 2000 and 1990, respectively. Simulations that include the BCA effect are denoted in a similar manner but have the suffix S. Δ denotes differences between simulations, '$_e$' changes from changing emissions based on economic activity (different time periods) and '$_{ce}$' changes from both climate and emissions. ΔBCEP (BC Emission changes for Present-day) represents changes due to differences between the Beig and Bond emissions for BC for present-day (2000) climate and emissions. For future climate change impacts ΔBCIEF (BC Indian Emissions for the Future) denotes differences between using BC emissions for 2010 and 2000 (BCISCF - $BCIS_c$) for the Beig emissions.

Annual surface distributions for sulfates, OM, BC from fossil/bio-fuel (BCF) and biomass

sources for BCI_0 indicate high sulfate and BCF concentrations over India (Fig.S1). Average values of BCF over India (4° to 40° N and 65° to 105° E) are 2.03 μgm^{-3} using the Beig emissions versus 1.05 μgm^{-3} using the Bond emissions. For $\Delta BCI_e/\Delta BCB_e$ (Fig.S1), sulfates decrease over Europe and North America but increase over Asia (notably over China, India and the Middle East). Changes to OM are mainly from biomass emissions and are similar to changes to BC from biomass. Like sulfates, BCF increases over Asia compared to the decrease observed over the Europe and North America.

For BCF, differences between ΔBCI_e and ΔBCB_e are mainly from the large change in BC emissions from India: 46% increase for the Beig emissions versus 14% increase for the Bond emissions. The annual average instantaneous radiative forcings for aerosols are given in Table S1. While other aerosol DE values are similar we obtain a factor of 2.6 increase in BCF forcing (for a factor of 2 increase in BCF emissions) for ΔBCI_e compared to ΔBCB_e. Thus, the total DE is greater for ΔBCI_e (0.12 Wm^{-2}) compared to ΔBCB_e (-0.16 Wm^{-2}). For the IE we obtain values of 0.10/-0.30 Wm^{-2} for $\Delta BCI_e/\Delta BCB_e$ over India. The smaller value of the IE for ΔBCI_e comes from smaller changes to cloud liquid water path (LWP) and a decrease in total cloud cover (CC) compared to ΔBCB_e (See Table S2). Thus, the reduction in CC and LWP (similar to the semi-direct effect described by (*21–23*)) due to the heating effects of BCF outweigh the impacts from the IE. The positive aerosol forcings obtained for ΔBCI_e can have a strong impact on climate. For the rest of the discussion, we focus mainly on the heating effects of BCF on climate over the Indian region.

Table 2 indicates values simulated for net radiation at TOA (NR-TOA) and the surface (NR-sfc). NR-TOA for ΔBCI_e is positive (due to the enhanced BCF) compared to the negative value for ΔBCB_e, and NR-sfc is negative for both due to the overall aerosol load increases for both cases that reduces radiation that can reach the surface. The heating effects of BCF over the column are stronger for ΔBCI_e as indicated by the increased value for the atmospheric forc-

ing obtained. This decreases CC and snow/ice cover and precipitation is reduced compared to ΔBCB$_e$. For simulations with climate (SST) effects, (comparing ΔBCI$_c$ with ΔBCI$_e$) with warmer SSTs, CC increases. With increased clouds, NR-TOA decreases and snow-cover increases (atmospheric forcing is reduced).

With the addition of the impact of BC on snow/ice surfaces precipitation and CC actually decrease as does snow/ice cover. BCA forcings are 0.0/-0.02 Wm^{-2} for ΔBCIS$_{ce}$/ΔBCBS$_{ce}$. For '$_e$' only effects, these values are 0.03/-0.02 Wm^{-2} for ΔBCIS$_e$/ΔBCBS$_e$. With climate effects included, a reduction in precipitation results in less BC deposition on the surface and thus reduced snow albedo forcings. This is further confirmed by a small reduction in surface BCF amounts for the simulations with changes in climate. Relevant changes to snow/ice cover shown in Fig.1 are a decline of 0.97/1.1 (%) for ΔBCIS$_{ce}$/ΔBCBS$_{ce}$ and without any climate influence values are -0.86/-0.63 (%). The aerosol contribution to this decline is $\sim$90%/60% for the Beig/Bond emissions and the enhanced BCF from the Beig emissions result in a 36% decrease in snow/ice cover.

In general for '$_e$' only driven changes, with increased atmospheric forcing, snow/ice cover decrease (see Table S2). The spatial patterns of simulated decrease of snow/ice cover (near 30°N) and an increase to the northeastern side, similar to observations (Fig.S3) is mainly obtained with the Beig emissions as shown in Fig.'s 1 and 2 (top left panel). This pattern also coincides with the BCA forcings (Fig.S4) and warmer surface temperatures (Fig.S5). Although the snow/ice cover decline is less than indicated in observations and the BCA forcing is smaller than other modeling studies (*6, 15*), qualitative features do indicate a BC impact on snow/ice cover, obtained for the higher BCF emissions.

For the future (2000 to 2010) BCF emission increase, the model predicts that the geographic pattern of snow/ice cover change is reversed to some extent as shown in Fig.2. Despite the high BCA forcings for the future over the entire Himalayan-Hindu-Kush region (Fig.S4), the

temperature pattern (Fig.S5) is more consistent with the snow/ice cover changes indicating a stronger atmospheric heating influence from BCF. These may be related to the spatial distribution of BCF aerosols (higher BCF values are more concentrated near eastern/western India for ΔBCIEF/ΔBCEP) and the prevailing winds (Fig.S6) that show opposite signs for ΔBCIEF and ΔBCEP (more westerly for ΔBCIEF). For ΔBCIEF, the higher BCF amounts (51%) results in a decrease in snow/ice cover (-0.05%). If we include the climate effect (BCISCF-BCIS$_o$), snow/ice cover declines by 0.16%. (Note that these future changes are due to increased BCF aerosols only as the other aerosols are constant). Thus BCF contributions result in a 31% decrease in snow/ice cover for 2000 to 2010 similar to the 36% decrease obtained from differences between the Beig and Bond emissions for 1990 to 2000.

In addition to snow/ice cover changes we also examine changes in the summer (June to August) precipitation due to BCF aerosols in Fig. 2. We find an increase in summer precipitation for the eastern parts of India with a decline in most other areas from the increased BCF emissions for present-day climate (Year 2000). For the future projection, with an increase in BCF emissions the decrease is confined to the north-central and southern parts. For ΔBCI$_{ce}$ and ΔBCI$_e$ precipitation changes over most parts of India (Fig.S7) are similar to observed trends (*24*) for similar time periods (Fig.S8); however the simulated increase over eastern India/Bangladesh for ΔBCI$_{ce}$ is opposite to observed trends. Trends based on summer rainfall from the Indian Meteorological Department (IMD) data (*25*) for the 1990-2000 period indicate a decrease over much of central India but an increase over eastern India (Fig.S9). However, the number of stations in eastern and northern India are sparse compared to the southern parts (*25*). Using the same data-set but for the 1950-2000 time period an increase in extreme rainfall events was found for India but with no strong trend otherwise (*26*). Based on the uncertainty that exists with precipitation data, we suggest that the simulations with the Beig emissions best capture the decline over central India indicated by both observations and BC aerosols can influence extreme

rainfall events, as indicated by the strong increase over east India (Fig.2).

Although we do not preclude the influence of large-scale circulation on spatial patterns of precipitation or snow cover changes, our results indicate that aerosols and the enhanced Indian BCF aerosols in particular may be responsible for some of the observed patterns and trends in snow/ice cover and precipitation. The range in climate impacts from the two emission inventories examined provide an estimate of the expected uncertainty in climate change from aerosols for the last decade and illustrate future expected challenges from aerosols and BC emissions in particular. Preserving the present snow/ice cover on the third polar ice cap would require concerted efforts to reduce both GHGs and BC emissions from coal as well as transportation and residential cooking/heating sources.

References and Notes

1. Economist, *Economist* **June 5** (2008).

2. V. Ramanathan, G. Carmichael, *Nature Geoscience* **1**, 221 (2008).

3. S. Menon, J. Hansen, L. Nazarenko, Y. Luo, *Science* **297**, 2250 (2002).

4. M. Jacobson, *J. Geophys. Res.* **109**, doi:10.1029/2004JD004945 (2004).

5. J. Hansen, L. Nazarenko, *Proc. Natl. Acad. Sci.* **101**, 423 (2004).

6. M. Flanner, C. S. Zender, J. Randerson, P. Rasch, *J. Geophys. Res.* **112**, doi10.1029/2006JD008003 (2007).

7. D. Koch, *et al., J. Climate* **XX** (2009). In Press.

8. C. Venkataraman, G. Habib, A. Eiguren-Fernandez, A.H.Miguel, S. Friedlander, *Science* **307**, 1454 (2005).

9. S. Fernandes, N. Trautmann, D. Streets, C. Roden, T. Bond, *Global Biogeochem. Cycles* **21**, GB2019,doi:10.1029/2006GB002836 (2007).

10. V. Ramanathan, P. Crutzen, P. Lelieveld, A. Mitra, D. A. et al., *J. Geophys. Res.* **104**, 2223 (2001).

11. V. Ramanathan, *et al., Proc. Natl. Acad. Sci.* **102(15)**, 5326 (2005).

12. V. Ramanathan, *et al.*, *Nature* **448**, 575 (2007).

13. J. Bahadur, *Proc. Kathmandu Symposium on Snow and Glacier Hydrology.* **218** (1992).

14. B. Etienne, *et al.*, *Remote Sens. Env.* **108**, 327 (2007).

15. J. Ming, *et al.*, *Atmos. Chem. Phys.* **8**, 1343 (2008).

16. J. Goes, P. Thoppil, H. Gomes, J. Fasullo, *Science* **308**, 545 (2005).

17. Materials, methods are available as supporting material on Science Online .

18. T. C. Bond, *et al., J. Geophys. Res.* **109**, doi:10.1029/2003JD003697 (2004).

19. S. Sahu, G. Beig, C. Sharma, *Geophys. Res. Lett.* **35**, doi:10.1029/2007GL032333 (2008).

20. W. Cooke, C. Liousse, H. Cachie, J. Feichter, *J. Geophys. Res.* **2**, 045030 (1999).

21. A. S. Ackerman, *et al.*, *Nature* **288**, 1042 (2000).

22. S. Menon, *Ann. Rev. Environ. Resour.* **29**, 1 (2004).

23. S. Menon, A. Del Genio, *Evaluating the impacts of carbonaceous aerosols on clouds and climate. In Human-induced climate change:An interdisciplinary assessment* (Cambridge University Press, 2007). (M. Schlesinger et al., Eds.).

24. T. Mitchell, P. Jones, *Intl. J. Climatol.* **25**, 693 (2005).

25. M. Rajeevan, J. Bhate, J. Kale, B. Lal, *Current Sci.* **91**, 296 (2006).

26. B. Goswami, V. Venugopa, D. Sengupta, M. Madhusoodanan, P. Xavier, *Science* **314**, 1442 (2006).

27. G. A. Schmidt, R. Ruedy, J. E. Hansen, I. Aleinov, N. Bell et al., *J. Climate* **19**, 153 (2006).

28. D. Koch, J. Hansen, *J. Geophys. Res.* **110**, D04204,doi:10.1029/2004JD005296 (2005).

29. D. Koch, T. Bond, D. Streets, N. Unger, *Geophys. Res. Lett.* **34** (2007a). L05821,doi:10.1029/2006GL028360.

30. S. Menon, *et al.*, *J. Geophys. Res.* **113** (2008a). Doi:10.1029/2007JD009442.

31. S. Twomey, *Atmos. Environ.* **25**, 2435 (1991).

32. B. A. Albrecht, *Science* **245**, 1227 (1989).

33. S. Menon, L. Rotstayn, *Clim. Dyn.* **27**, 345 (2006).

34. S. Menon, *et al.*, *Envtl. Res. Lett.* **3** (2008b). 024004.

35. H. Morrison, A. Gettelman, *J. Climate* **21**, 3642 (2008).

36. U. Lohmann, *et al.*, *Atmos. Chem. Phys.* **7**, 3425 (2007).

37. U. Lohmann, J. Feichter, C. Chuang, J. Penner, *J. Geophys. Res.* **104**, 9169 (1999).

38. M. O. Andrea, P. Merlet, *Global Biogeochem. Cycles* **15**, 955 (2001).

39. N. Rayner, *et al.*, *J. Geophys. Res.* **108**, doi:10.1029/2002JD002670 (2003).

40. R. Armstrong, M. Brodzik, *National Snow and Ice Data Center* **Digital media** (2005).

41. This work was supported by the U.S. Department of Energy under Contract No. DE-AC02-05CH11231at Lawrence Berkeley National Laboratory and under Contract DE-AC52-07NA27344 at Lawrence Livermore National Laboratory. SM acknowledges support from the NASA MAP Program and the DOE Atmospheric Radiation Program and thanks Hugh Morrison (NCAR) and Igor Sednev (LBNL) for help with the cloud scheme used in the climate model.

Table 1: Description of simulations used for the study. All simulations use the Beig emissions unless otherwise indicated. Emissions from year 2000 are considered as present-day since these are the most current full suite of emission inventories available for the chemistry model. Sea-surface temperatures for 1993-2002 are warmer by 0.19K compared to 1975-84. Only black carbon emissions from fossil and biofuel are for 2010, the rest (sulfates, organic matter and black carbon from biomass) are from year 2000.

Simulation	Aerosols	Sea-surface/sea ice temperature	Processes treated
BCI_9	1990	1975-84	Aerosol Direct + Indirect effects
BCI_0	2000	1975-84	Like BCI_9
BCI_c	2000	1993-2002	Like BCI_9
BCB_9	1990	1975-84	Like BCI_9 but with Bond's emissions
BCB_0	2000	1975-84	Like BCB_9
BCB_c	2000	1993-2002	Like BCB_9
$BCIS_9$	1990	1975-84	Like BCI_9 + BC deposition on snow/ice
$BCIS_0$	2000	1975-84	Like $BCIS_9$
$BCIS_c$	2000	1993-2002	Like $BCIS_9$
$BCBS_9$	1990	1975-84	Like $BCIS_9$ but with Bond's emissions
$BCBS_0$	2000	1975-84	Like $BCBS_9$
$BCBS_c$	2000	1993-2002	Like $BCBS_9$
BCISCF	2010	1993-2002	Like $BCIS_c$

Table 2: Annual average differences in TOA net radiation (NR-TOA), surface net radiation (NR-Sfc), atmospheric forcing, snow/ice cover, precipitation and total cloud cover for the Indian region (4°-40° N and 65°-105° E) for the various simulations.

Variable	ΔBCI$_e$	ΔBCB$_e$	ΔBCI$_c$	ΔBCB$_c$
NR-TOA (Wm^{-2})	0.14	-0.42	-1.31	- 1.74
NR-Sfc (Wm^{-2})	-1.11	-1.22	-0.51	0.22
Atmospheric forcing (Wm^{-2})	1.25	0.80	-0.80	-1.96
Snow/ice cover (%)	-0.46	0.46	0.33	0.54
Precipitation (mm/day)	-0.08	0.05	0.08	-0.01
Total cloud cover (%)	-0.60	0.44	-0.10	-0.26

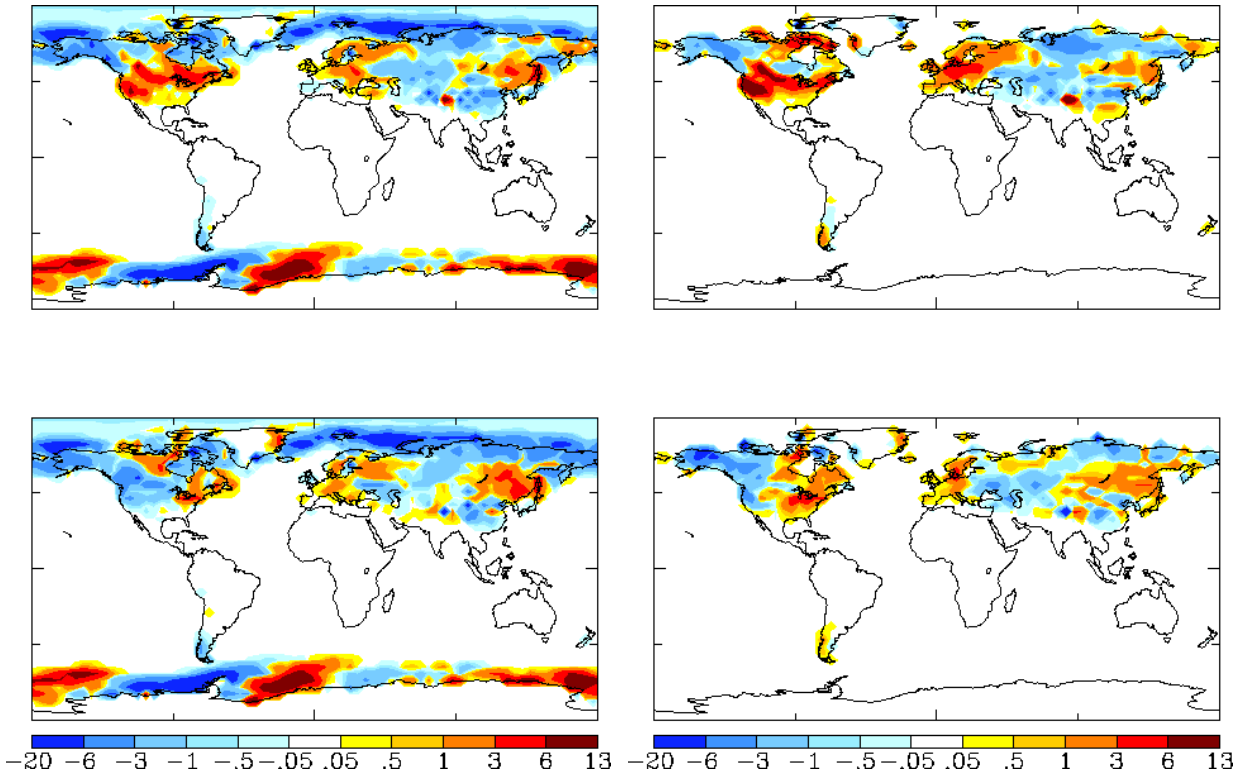

Figure 1: Average difference in annual snow/ice cover (%) for differences in emissions between 2000 and 1990 with (left panel) and without (right panel) the climate influence. The top panels represent ΔBCI_{ce} (left) and ΔBCI_{e} (right) and the bottom panels represent ΔBCB_{ce} (left) and ΔBCB_{e} (right).

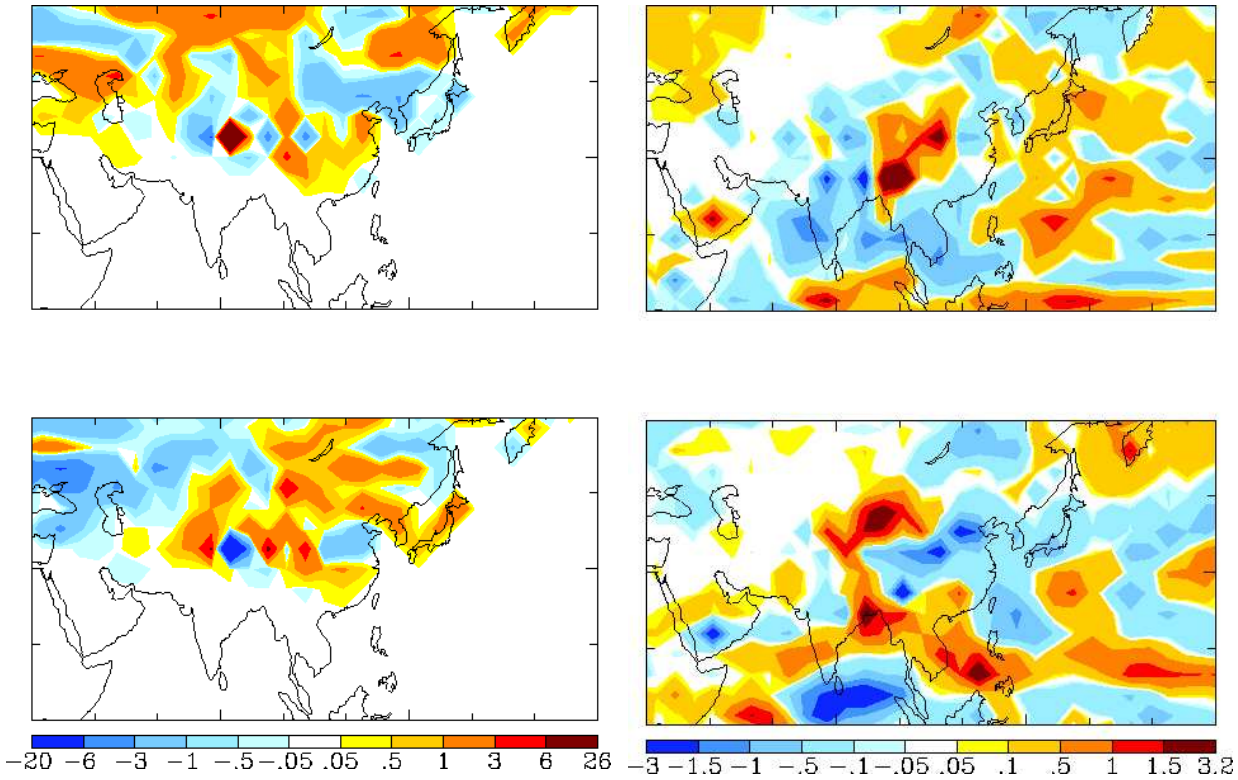

Figure 2: Average difference in annual snow/ice cover (%) (left panel) and June-July-August precipitation (mm/d) (right panel). The top panels represent differences due to black carbon used in the Beig and Bond emissions for present-day (Year 2000) (ΔBCEP) and the bottom panels represent future changes (2000 to 2010) from black carbon for the Beig emissions (ΔBCIEF).

Supplementary text: Material and Methods

The Goddard Institute for Space Studies climate model, ModelE (4°x5° horizontal resolution and 20 vertical layers) used in this study is described in detail in (*27*). The aerosol chemistry/transport model (*28, 29*) includes sulfate chemistry and source terms for organic matter (OM includes organic carbon (OC) and associated species via OM = 1.3XOC) and black carbon (BC) aerosols that are transported and subject to the same physical processes (wet/dry deposition) as sulfates. Both sea-salt and dust are treated as natural emissions, and their anthropogenic fraction is assumed to be zero, based on the considerable uncertainty that exists

in determining their anthropogenic fractions. We also include schemes to treat aerosol-cloud interactions, the so-called aerosol indirect effect (*23, 30*). An increase in aerosols can increase cloud droplet number concentration (CDNC) and reduce cloud droplet sizes, thereby increasing cloud optical depth and reflectivity if the cloud liquid water content is unchanged (*31*). These reduced droplet sizes also inhibit precipitation, increasing cloud liquid water path (LWP) and optical depth and hence cloud reflectivity (*32*).

Although the treatment of the indirect effect is similar in concept to that in (*30, 33, 34*), we include a different treatment to calculate CDNC and ice crystal number. We use a prognostic equation to calculate CDNC, based on (*35*). This includes both sources (newly nucleated CDNC) and sinks (CDNC loss from autoconversion, contact and immersion freezing) for CDNC. The nucleation term (Q_{nucl}) [m^{-3} s^{-1}] for CDNC is from (*36*) given as:

$$Q_{nucl} = max\left[\frac{1}{\Delta t}\left(0.1\left(\frac{N_a w}{w + \alpha N_a}\right)^{1.27} - CDNC_{old}\right), 0\right] \quad (1)$$

where N_a is the aerosol concentration obtained from the aerosol mass as in (*37*), ω is the vertical velocity obtained by taking into account model grid-mean velocity and sub-grid turbulence, and α = 0.023 cm^4 s^{-1} is a constant obtained from aircraft measurements. Δt is the time step in the model and $CDNC_{old}$ is the CDNC from the previous time step. For ice crystal concentrations we include both heterogeneous freezing via immersion and nucleation by deposition/condensation freezing following the treatment described in more detail by (*35*). However, aerosols do not directly affect ice crystal nucleation since considerable uncertainty exists in determining the fraction of aerosol species that may serve as ice nuclei.

To represent BC deposition on snow and ice surfaces and modifications to snow/ice albedo we use the treatment described in more detail by (*7*). Essentially BC concentrations in the top layer of snow (land and sea ice) are used to calculate the albedo reduction on snow grains with sizes varying from 0.1 to 1 mm. The forcing is then obtained by calculating the instantaneous

TOA radiative flux with and without the BC impact on snow/ice albedo when the radiation routine is called. A similar method is used to calculate the forcing for the aerosol direct effect. The aerosol mass, optical properties and the aerosol direct effect have been extensively evaluated in (*7*). The aerosol indirect effect is calculated from changes to the net cloud forcing obtained from the difference between total and clear skies for each call to the radiation routine.

For emissions, we use the sulfur emissions from the Emission database for global atmospheric research (V3.2 1995). Biomass emissions for all aerosols (sulfates and carbonaceous aerosols) are based on the Global Fire Emissions Database (v1) carbon estimates with emission factors from (*38*). More details on emissions, including natural emissions used are described in (*7*). Climatological (monthly varying) sea surface temperatures and sea ice extent are based on averages from 1975-1984 or from 1993-2002 (*39*). Model simulations are run for 63 months and averages for the last five years are given, allowing for a spin-up time of three months. Significance of values represented in the analysis for differences between simulations are discussed in more detail in (*34*).

References and Notes

1. Economist, *Economist* **June 5** (2008).

2. V. Ramanathan, G. Carmichael, *Nature Geoscience* **1**, 221 (2008).

3. S. Menon, J. Hansen, L. Nazarenko, Y. Luo, *Science* **297**, 2250 (2002).

4. M. Jacobson, *J. Geophys. Res.* **109**, doi:10.1029/2004JD004945 (2004).

5. J. Hansen, L. Nazarenko, *Proc. Natl. Acad. Sci.* **101**, 423 (2004).

6. M. Flanner, C. S. Zender, J. Randerson, P. Rasch, *J. Geophys. Res.* **112**, doi10.1029/2006JD008003 (2007).

7. D. Koch, *et al., J. Climate* **XX** (2009). In Press.

8. C. Venkataraman, G. Habib, A. Eiguren-Fernandez, A.H.Miguel, S. Friedlander, *Science* **307**, 1454 (2005).

9. S. Fernandes, N. Trautmann, D. Streets, C. Roden, T. Bond, *Global Biogeochem. Cycles* **21**, GB2019,doi:10.1029/2006GB002836 (2007).

10. V. Ramanathan, P. Crutzen, P. Lelieveld, A. Mitra, D. A. et al., *J. Geophys. Res.* **104**, 2223 (2001).

11. V. Ramanathan, *et al., Proc. Natl. Acad. Sci.* **102(15)**, 5326 (2005).

12. V. Ramanathan, *et al., Nature* **448**, 575 (2007).

13. J. Bahadur, *Proc. Kathmandu Symposium on Snow and Glacier Hydrology.* **218** (1992).

14. B. Etienne, *et al., Remote Sens. Env.* **108**, 327 (2007).

15. J. Ming, *et al., Atmos. Chem. Phys.* **8**, 1343 (2008).

16. J. Goes, P. Thoppil, H. Gomes, J. Fasullo, *Science* **308**, 545 (2005).

17. Materials, methods are available as supporting material on Science Online .

18. T. C. Bond, *et al., J. Geophys. Res.* **109**, doi:10.1029/2003JD003697 (2004).

19. S. Sahu, G. Beig, C. Sharma, *Geophys. Res. Lett.* **35**, doi:10.1029/2007GL032333 (2008).

20. W. Cooke, C. Liousse, H. Cachie, J. Feichter, *J. Geophys. Res.* **2**, 045030 (1999).

21. A. S. Ackerman, *et al., Nature* **288**, 1042 (2000).

22. S. Menon, *Ann. Rev. Environ. Resour.* **29**, 1 (2004).

23. S. Menon, A. Del Genio, *Evaluating the impacts of carbonaceous aerosols on clouds and climate. In Human-induced climate change:An interdisciplinary assessment* (Cambridge University Press, 2007). (M. Schlesinger et al., Eds.).

24. T. Mitchell, P. Jones, *Intl. J. Climatol.* **25**, 693 (2005).

25. M. Rajeevan, J. Bhate, J. Kale, B. Lal, *Current Sci.* **91**, 296 (2006).

26. B. Goswami, V. Venugopa, D. Sengupta, M. Madhusoodanan, P. Xavier, *Science* **314**, 1442 (2006).

27. G. A. Schmidt, R. Ruedy, J. E. Hansen, I. Aleinov, N. Bell et al., *J. Climate* **19**, 153 (2006).

28. D. Koch, J. Hansen, *J. Geophys. Res.* **110**, D04204,doi:10.1029/2004JD005296 (2005).

29. D. Koch, T. Bond, D. Streets, N. Unger, *Geophys. Res. Lett.* **34** (2007a). L05821,doi:10.1029/2006GL028360.

30. S. Menon, *et al.*, *J. Geophys. Res.* **113** (2008a). Doi:10.1029/2007JD009442.

31. S. Twomey, *Atmos. Environ.* **25**, 2435 (1991).

32. B. A. Albrecht, *Science* **245**, 1227 (1989).

33. S. Menon, L. Rotstayn, *Clim. Dyn.* **27**, 345 (2006).

34. S. Menon, *et al.*, *Envtl. Res. Lett.* **3** (2008b). 024004.

35. H. Morrison, A. Gettelman, *J. Climate* **21**, 3642 (2008).

36. U. Lohmann, *et al.*, *Atmos. Chem. Phys.* **7**, 3425 (2007).

37. U. Lohmann, J. Feichter, C. Chuang, J. Penner, *J. Geophys. Res.* **104**, 9169 (1999).

38. M. O. Andrea, P. Merlet, *Global Biogeochem. Cycles* **15**, 955 (2001).

39. N. Rayner, *et al.*, *J. Geophys. Res.* **108**, doi:10.1029/2002JD002670 (2003).

40. R. Armstrong, M. Brodzik, *National Snow and Ice Data Center* **Digital media** (2005).

Table 3: Annual average instantaneous shortwave radiative forcings at the tropopause averaged over India (4°-40° N and 65°-105° E) for the various simulations. OM refers to organic matter, BCB to black carbon from biomass sources and BCF to black carbon from fossil/bio-fuel sources. Global values are given in parenthesis. Also included are values for the aerosol indirect effect (estimated from changes to the net (shortwave + longwave) cloud forcing), cloud liquid water path (LWP) and total cloud cover. All units are in Wm^{-2} unless otherwise indicated.

Species	BCI_0	BCB_0	ΔBCI_e	ΔBCB_e
Sulfate	-1.12 (-0.86)	-1.11 (-0.86)	-0.13 (0.04)	-0.15 (0.03)
OM	-1.19 (-0.47)	-1.19 (-0.46)	-0.11 (-0.02)	-0.11 (-0.02)
BCB	0.084 (0.14)	0.085 (0.14)	0.003 (0.008)	0.004 (0.009)
BCF	1.29 (0.31)	0.76 (0.27)	0.36 (0.03)	0.10 (0.005)
Aerosol direct effect	-0.94 (-0.88)	-1.46 (-0.91)	0.12 (0.06)	-0.16 (0.02)
Liquid water path (gm^{-2})	43.33 (47.88)	44.78 (48.05)	0.02 (0.056)	0.46 (0.22)
Cloud cover (%)	50.51 (57.42)	51.33 (57.43)	-0.60 (0.02)	0.44 (0.48)
Aerosol indirect effect	-13.9 (-16.6)	-14.7 (-16.7)	0.10 (-0.10)	-0.30 (-0.11)
Total aerosol effect	-14.8 (-17.5)	-16.2 (-17.6)	0.22 (-0.04)	-0.46 (-0.09)

Table 4: Annual average atmospheric forcing (Wm^{-2}) and snow/ice cover ($\%$) changes for the various simulations.

Variable	ΔBCI_e	ΔBCB_e	$\Delta BCIS_e$	$\Delta BCBS_e$
Atmospheric forcing (Wm^{-2})	1.25	0.80	1.97	1.92
Snow/ice cover ($\%$)	-0.46	0.33	-0.86	-0.63

Figure 3: Map of the Indian subcontinental region showing the Himalayas. The Himalayan-Hindu-Kush region extends 3500 km from Afghanistan to Myanmar (Burma) (from http://www.worldatlas.com).

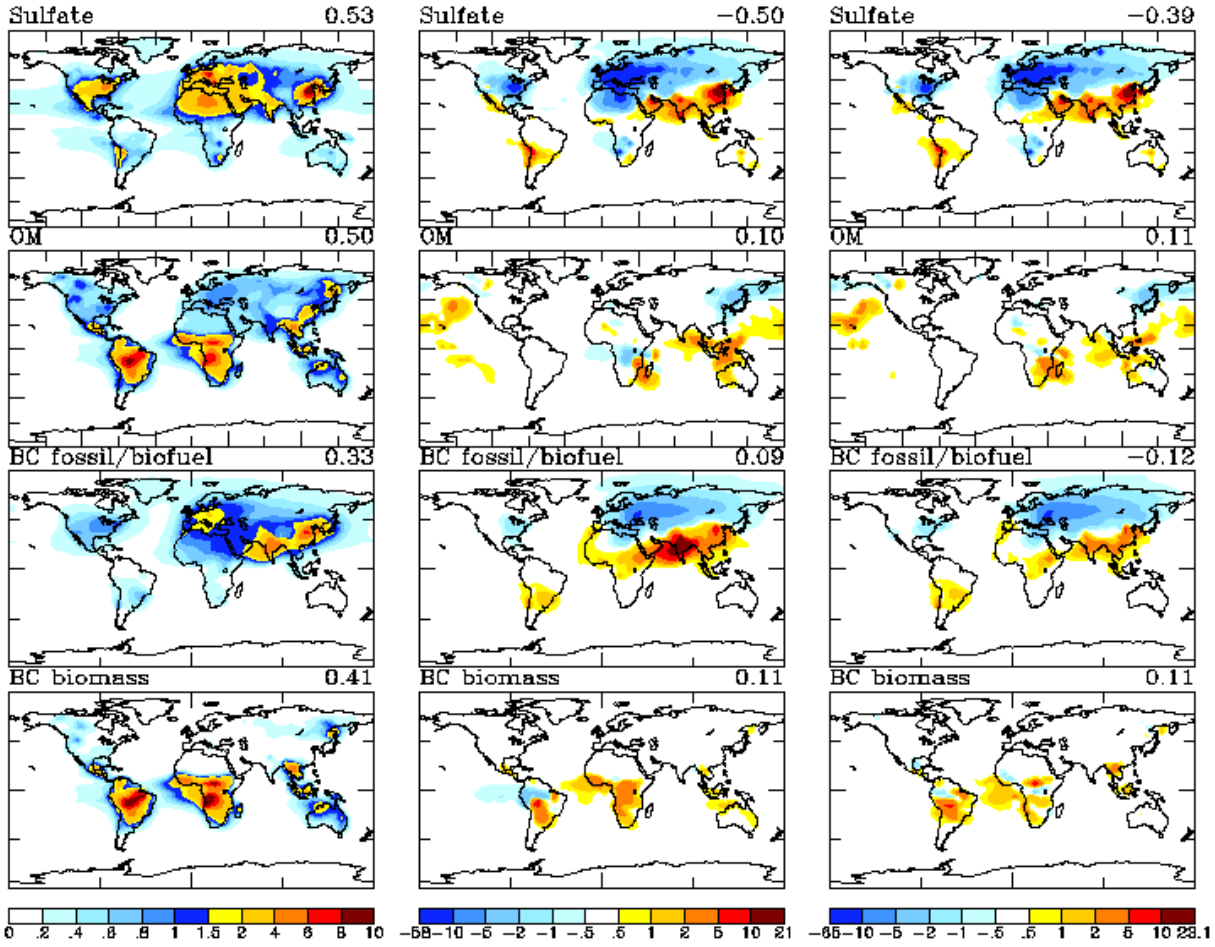

Figure 4: Average annual surface layer mass concentrations in (μgm^{-3}) for sulfate and organic matter (OM) from all sources and black carbon (BC) from fossil/bio-fuel and biomass sources for simulations BCI_0 (left panel), ΔBCI_e (middle panel) and ΔBCB_e (right panel). Values for BC in the left panel are multiplied by a factor of 10 to facilitate comparison with other aerosols. Global values are listed on the rhs. Note that although only the BC emissions from fossil/bio-fuel sources are different between the simulations used here (ΔBCI_e andΔBCB_e), small differences in concentrations for sulfates or OM or BC from biomass do occur, most notably for sulfate. These are due to feedbacks to aerosols (especially for the sulfur chemistry cycle) from the various physical processes represented (wet scavenging, radiative heating from BC aerosols, dry deposition, etc.) and associated cloud changes.

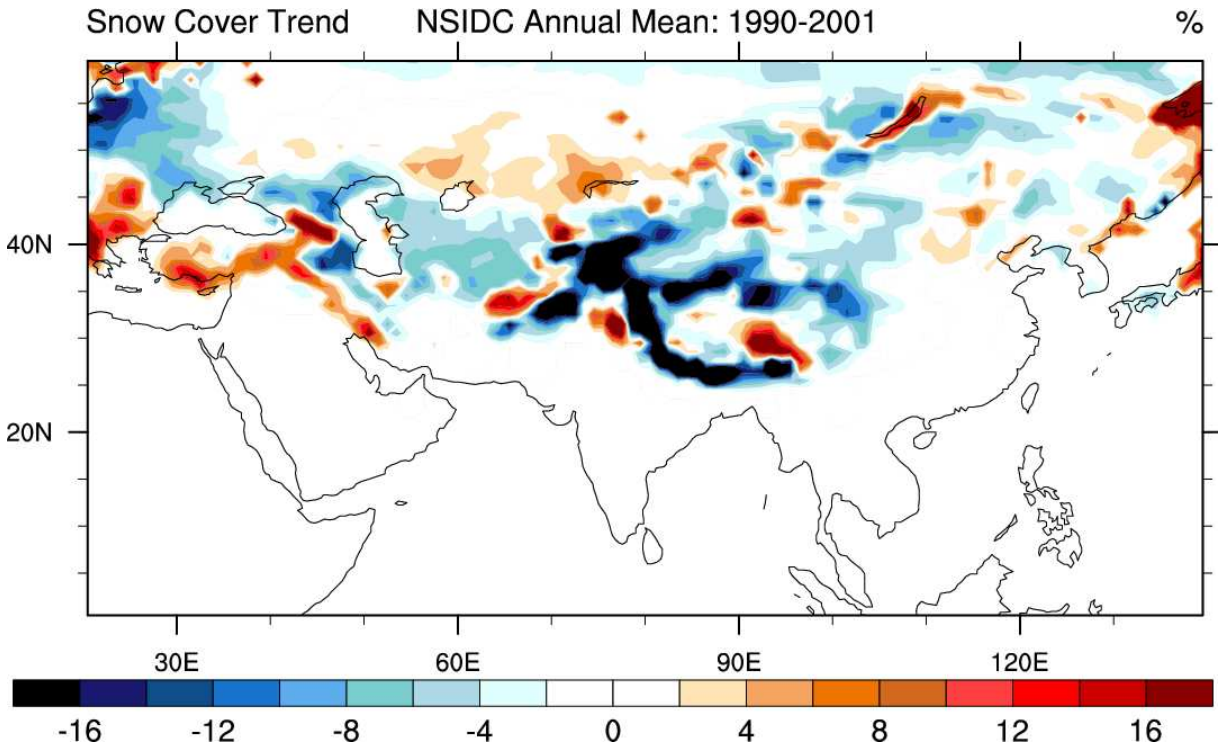

Figure 5: Trend in annual linear snow cover (expressed as % per decade) from 1990 to 2001 as obtained from the National Snow and Ice Data Center (NSIDC) EASE_Grid weekly snow cover and sea ice extent dataset (*40*). Trend is based on a least-square linear fit.

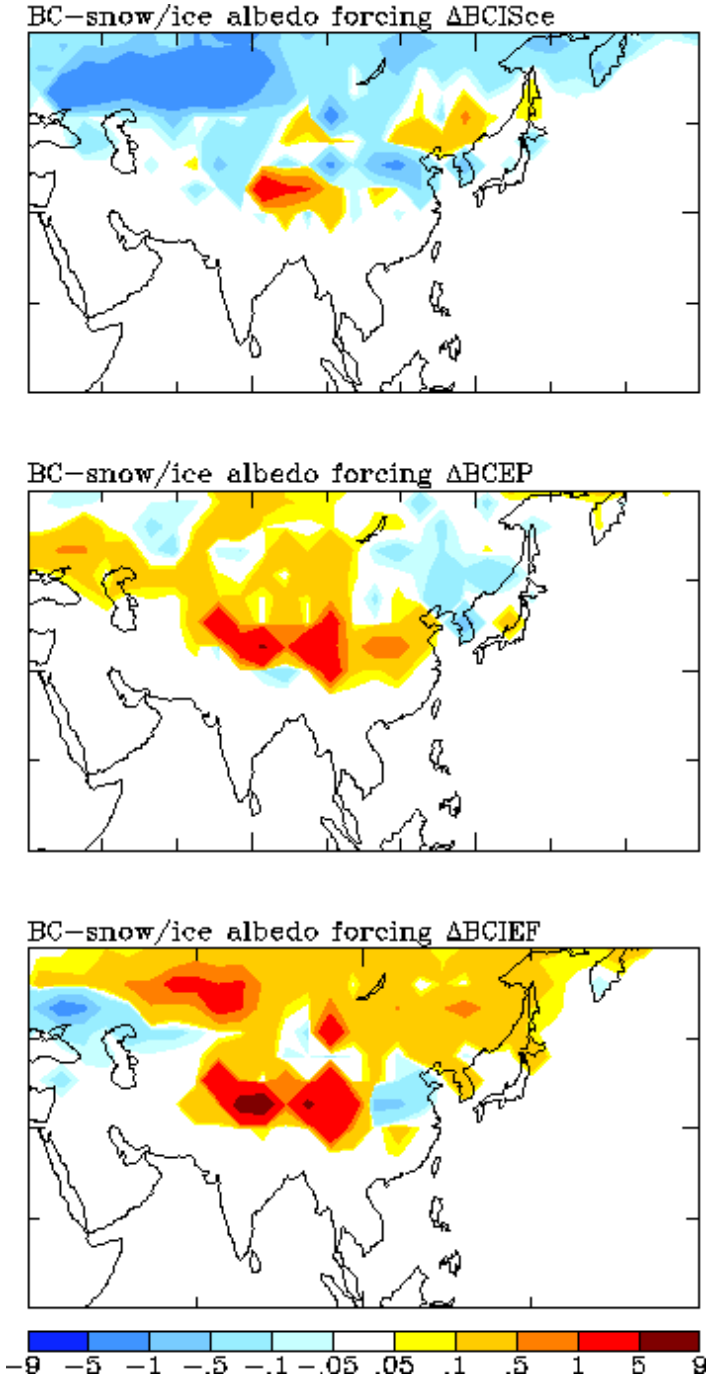

Figure 6: Differences in annual average forcing (0.1 Wm^{-2}) from changes to snow/ice albedo due to black carbon deposition on snow/ice surfaces for the various simulations.

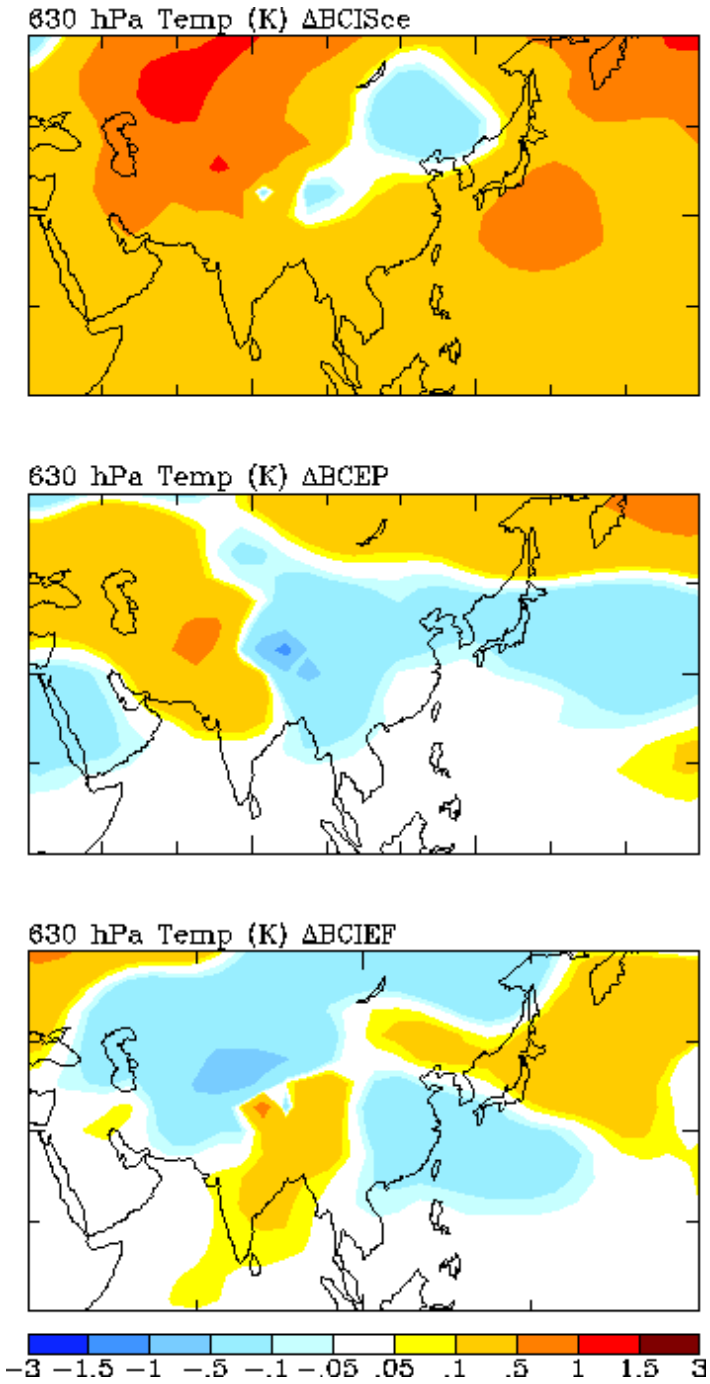

Figure 7: Similar to Fig.4 but for temperature at 630 hPa. We use temperatures at 630 hPa (∼4000 m) that are indicative of surface temperatures for the high mountain ranges in the Himalayan-Hindu-Kush region that vary in height between 3 to 5 km (*12*).

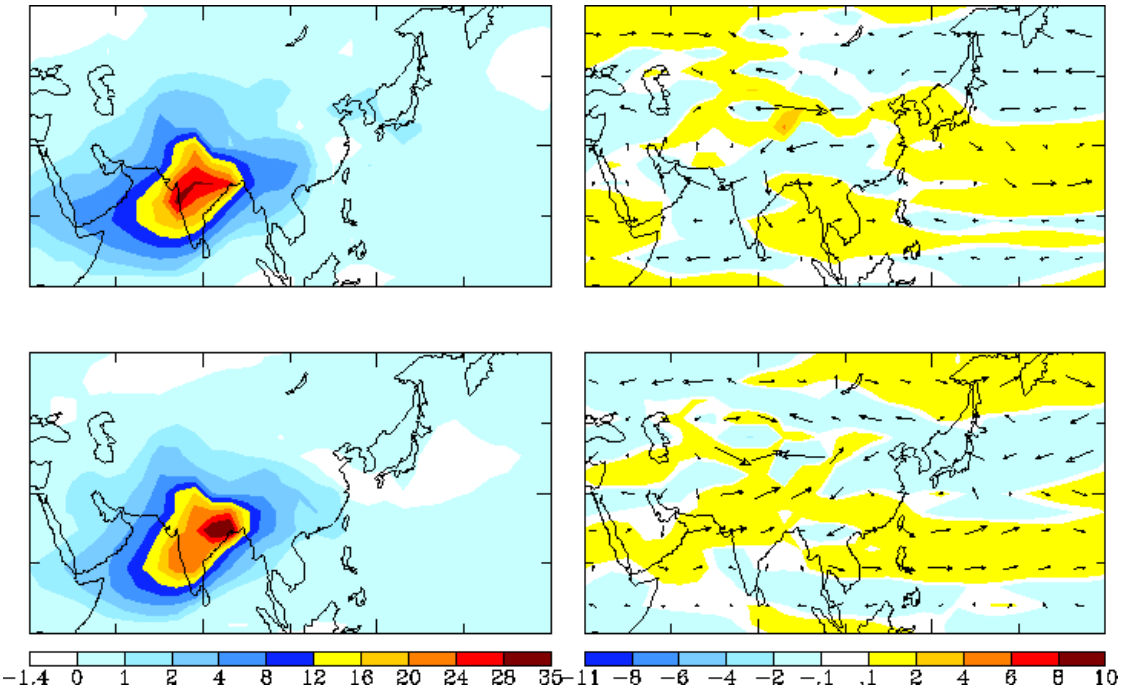

Figure 8: Differences in annual average black carbon (BC) aerosols from fossil and bio-fuel sources (left panel) and wind fields at 630hPa (right panels). The top panels represent differences due to black carbon used in the Beig and Bond emissions for present-day (Year 2000) (ΔBCEP) and the bottom panels represent future changes (Year 2010 - Year 2000) from black carbon for the Beig emissions (ΔBCIEF).

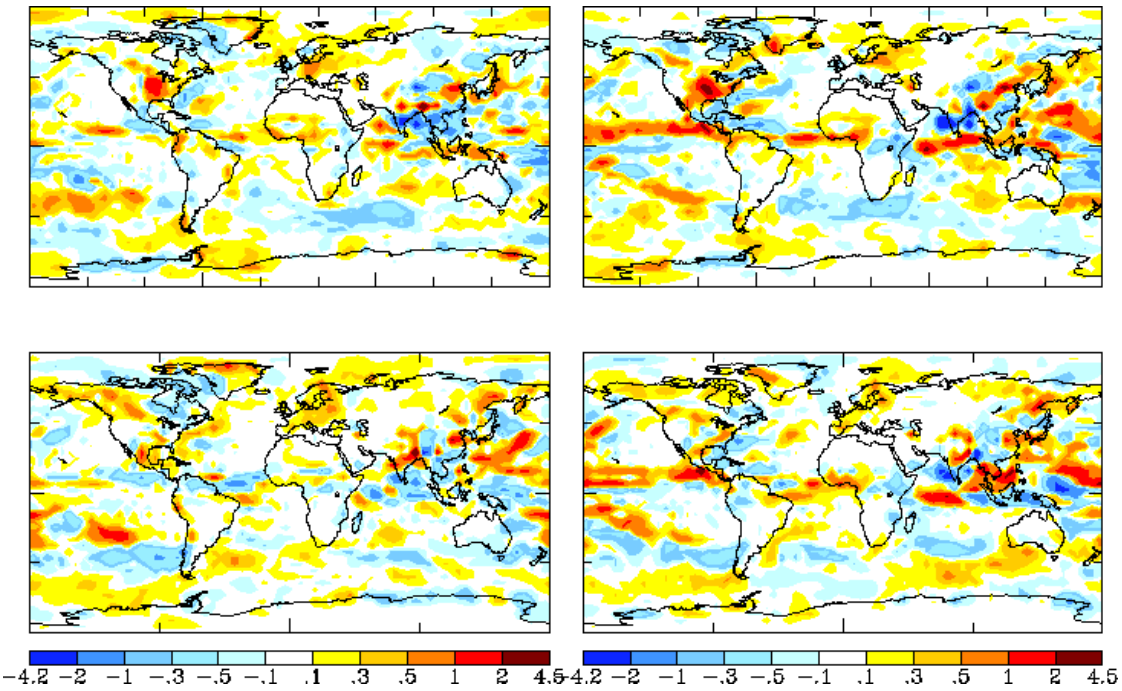

Figure 9: Average difference in summer (June to August) precipitation for differences in emissions between 2000 and 1990 with (left panel) and without (right panel) the climate influence. The top panels represent $\Delta\mathrm{BCI}_{ce}$ (left) and $\Delta\mathrm{BCI}_{e}$ (right) and the bottom panels represent $\Delta\mathrm{BCB}_{ce}$ (left) and $\Delta\mathrm{BCB}_{e}$ (right).

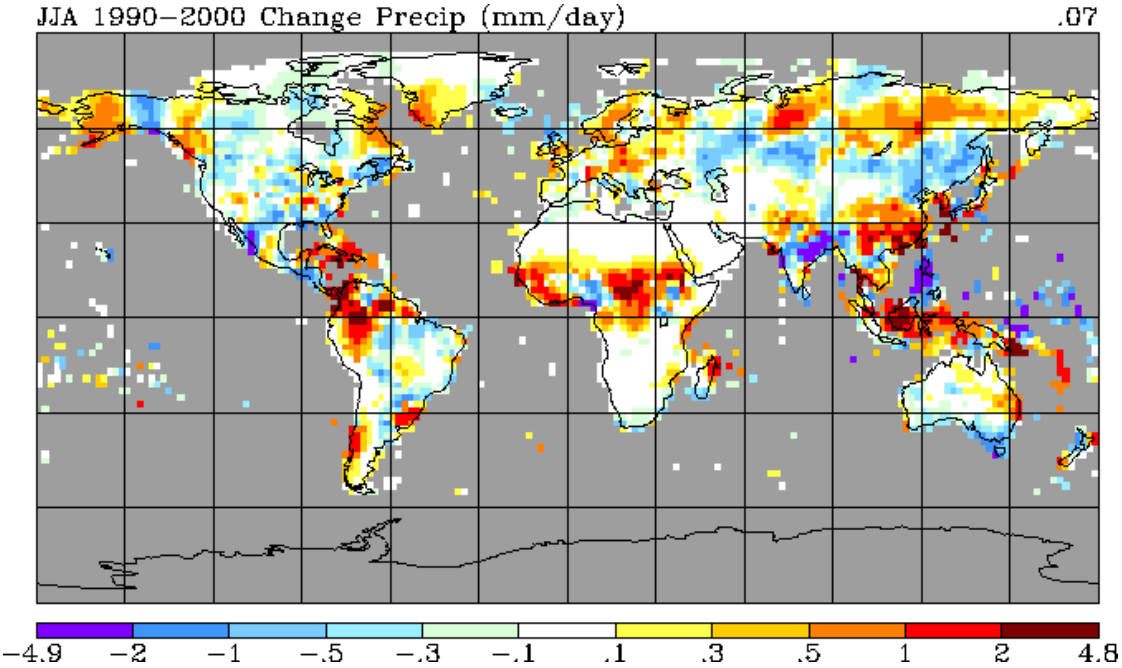

Figure 10: Trend in summer (June to August (JJA)) precipitation between 1990 and 2000 using observations from CRU TS2.0 (*24*) available at http://data.giss.nasa.gov/precip_cru/maps.html. Global mean change is given on the r.h.s. of the figure.

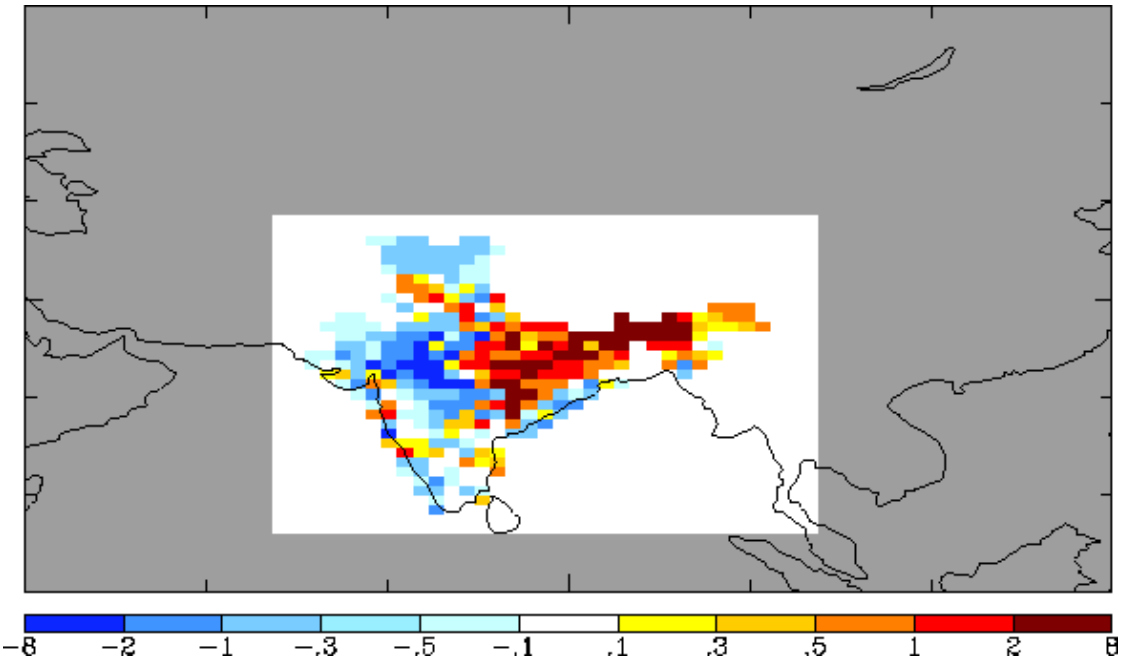

Figure 11: Trend in summer (June to August) precipitation between 1990 and 2000 using observations from the Indian Meteorological Department (IMD) data (*25*).